

A2-type granitoids in anorogenic settings of Tusham Ring Complex: New concept, relevant to existence of the Malani Supercontinent

Naresh Kumar¹ and Naveen Kumar^{*2}

¹Assistant Professor, Department of Geology, Kurukshetra University, Kurukshetra, 136119, India

^{*2}Research Scholar, Department of Geology, Kurukshetra University, Kurukshetra, 136119, India

*Corresponding author's email: naveenphdkuk@gmail.com

Submitted date: 18/10/2019 Accepted date: 10/10/2020 Published online: 30/11/2020

Abstract

This contribution discusses A2-type (sub-type of A-type granitoids) magmatic rocks which were emplaced in confusing tectonic settings and identified with mixed crust-mantle geochemistry. The Tusham Ring Complex (TRC), in the northern part of the Trans-Aravalli Block (TAB), is characterized by volcano-plutonic association, and belongs to Neoproterozoic Malani Igneous Suite (MIS). The rock-types exposed in TRC include intrusions of grey granite, pink granite, grayish green granite, biotite granite and ring dykes, extrusions of rhyolite, quartz porphyry and tuff, and some meta-sedimentary rocks (quartzite, quartz-mica schist and schorl rock). Field studies, petrography and geochemistry propose that the magmatic rocks have close linkage with the Malani anorogenic felsic magmatism and are i.e. a part of the Neoproterozoic Malani Supercontinent. The magmatic evolution established a close association in space and time between the explosive acid lava and high-level granite that form distinct ring structure and radial dykes in NW Indian shield. Trace elements and their ratio suggest that these are formed in A2-type tectono-magmatic environment which is an interesting subject of debate among modern petrologist.

Keywords: Tusham Ring Complex; Malani Igneous Suite; A2-type granitoid; Peraluminous.

1. Introduction

Previous workers demonstrated that the Malani rocks in the Tusham Ring Complex (TRC) are underlain by the Delhi quartzite and overlain by Vindhyan arenaceous sediments (Crawford and Compston, 1970; Pareek, 1981). They also advocated that at the end of orogenic cycle in the Aravalli craton, anorogenic, intraplate magmatism, took place in an extensional tectonic regime. Commonly referred to as the Malani Igneous Suite (MIS), this magmatism comprises mafic and felsic volcanic and plutonic rocks covering large area in W Rajasthan and SE Pakistan. The regional geological map is constructed to show the important exposures of Malani terrain (Fig. 1a). The simplified geological map of TRC includes the isolated granitic massifs and associated felsic volcanics around Tusham Ring Complex in southwestern Haryana state of the Indian shield (Fig. 1b). The volcano-plutonic ring structure, radial dykes and NE-SW trending structural lineaments in TRC, which are indicative of extensional tectonic environment, confirm the TAB separation from East Gondwana, about 732 Ma ago (Eby and

Kochhar, 1990; Kochhar, 2015; Sharma and Kumar, 2017; Kumar et al., 2019; Sharma et al., 2019). This magmatic period is also assigned to the major Pan-African thermo-tectonic event which is closely related with acid magmatism of alkali granites and co-magmatic rhyolites in the TAB of the Indian shield, central Iran, Arabian shield, Madagascar, South China, Somalia and Seychelles, which have been taken to suggest the existence of the Malani Supercontinent (Kochhar, 2015; Wang et al., 2017; Sharma and Kumar, 2017; Sharma et al., 2019; Kumar et al., 2019, 2020). The volcanic and plutonic rocks constituting the MIS, along with TRC, are genetically attributed to melting within the flattening head of mantle plume and owe their origin to hot spot magmatism (Kochhar, 2015). Despite intensive research work which covers mostly petrology and geochemistry of rock-types, no consensus exists on the phase petrology and magmatic evolution of A2-type granitoids of TRC.

2. Field observations and petrography

Based on field evidences, the acid volcano-plutonic rocks of TRC can be divided

into three stages of magmatism, i.e., rhyolite as first phase, granite as second phase, and felsic dykes as third and last phase. Some important field photographs are captured to show the variations in lithologies of the TRC (Fig. 2a-d). Petrographically, the TRC granites show hypidiomorphic, granophyric and microgranophyric textures, whereas the rhyolites show porphyritic, granophyric, vitrophyric, glomeroporphyritic, aphyritic, spherulitic and perlitic textures. Some important rock-textures are sketched to show the mineralogical inter-relationships (Fig. 3a-f). Rhyolites of grey and pink color, consist of embayed quartz, sanidine, plagioclase, biotite as essential mineralogy whereas magnetite, zircon, apatite, monazite, fluorite, chlorite and rutile as accessory mineralogy, whereas granites of pink and grey colored consist of quartz, K-feldspar (perthite, orthoclase), plagioclase (albite to andesine), biotite and muscovite as essential minerals whereas apatite, zircon, chlorite, fluorite, monazite, titanite, rutile and allanite as accessory minerals. The back-scattered electron (BSE) imaged recorded during EPMA, suggest the presence of halogens as volatile phase (especially, F and Cl) that is very important

factor in hydrothermal activity in Northwestern peninsular India (Kumar et al., 2020). It can also be assumed that the studied granitoids might be generated from halogen-enriched magma. The ongoing field observations and petro-mineralogical relationships are closely matching with the A2-type granitoids of palaeo-existed Malani Supercontinent (Kochhar, 2015).

3. Analytical methods

A large number of samples (80), including granite and rhyolite, were collected for detail petrographical and geochemical studies. Thin sections of representative samples were studied by optical microscope. The petrographical study and whole-rock geochemical analysis were carried out at the Wadia Institute of Himalayan Geology (WIHG), Dehradun, India. To describe the geochemical characteristics of investigating areas, representative samples of various types of granites and rhyolites from TRC were selected for geochemical analysis. Major oxides and selected trace element data were determined from powder pellets by X-Ray Fluorescence Spectrometer.

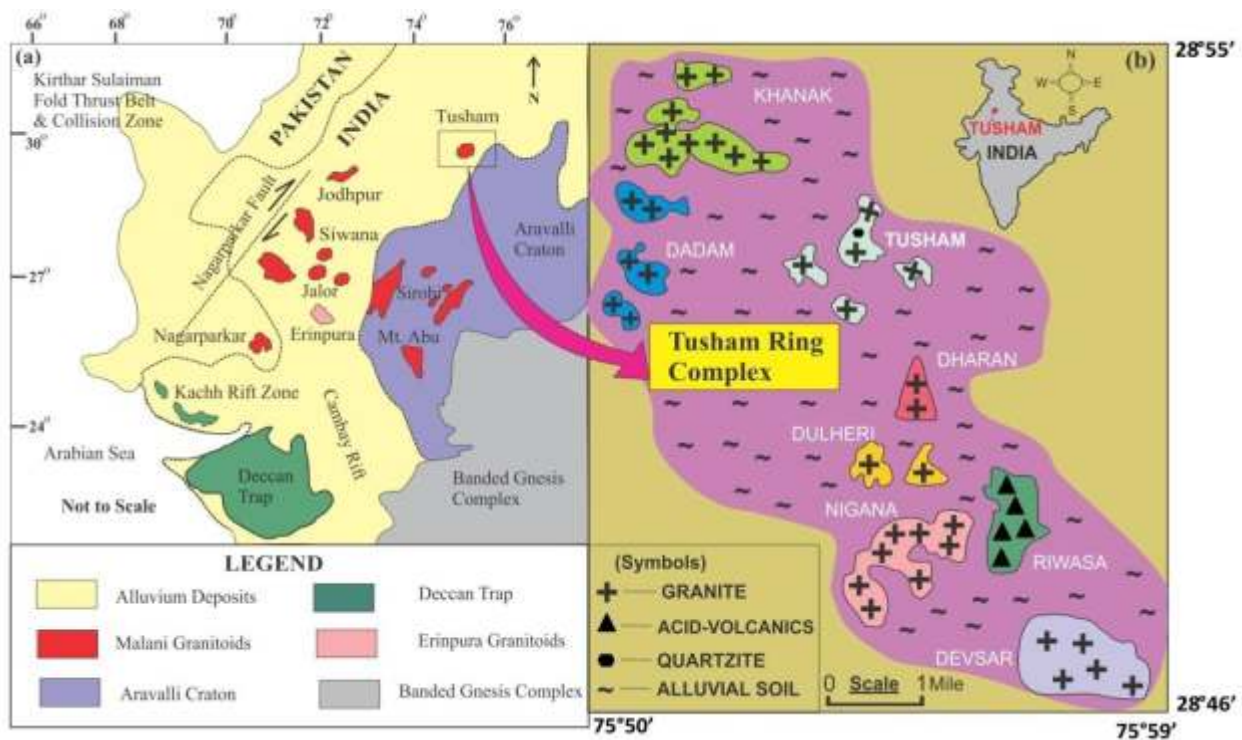


Fig. 1. (a) Regional geological map of the Malani Igneous Suite exposed in NW Indian shield and SE Pakistan (modified after, Shakoor et al., 2019). (b) Simplified geological map of Tusham Ring Complex (modified after, Kochhar, 1984; Kumar et al., 2020).



Fig. 2. (a) Mafic enclave (about 13 cm in size) in porphyritic rhyolite of Riwasa area of TRC. (b) A close view of grey rhyolite with xenolith (about 5 cm in size) in Riwasa volcanics. (c) The picture shows consolidated joints in light grey granite of Nigana massifs. (d) A close view of light pink granite with xenoliths (about 11 cm in size) of intermediate composition in Nigana massifs.

Loss-on-ignition was determined by heating a separate aliquot (0.5 gm rock powder) of each representative sample at 10000 C for 5 hrs. Rare earth elements (REE) of the samples were determined in the same institute by Inductively Couple Plasma-Mass Spectrometer using the open system rock digestion method. Analytical precision for major elements is well within ± 2 to 3% and ± 5 to 6% for trace elements. Accuracy of rare earth elements ranges from 2 to 12% and precision varies from 1 to 8%. To study mineral chemistry of acid magmatic rocks of TRC, 14 representative thin-slides of granites (11) and rhyolites (3) were selected. The analytical work was carried out on the Electron Probe Micro Analyzer (EPMA) CAMECA SXFive instrument at DST-SERB National Facility, Department of Geology (Center of Advanced Study), Institute of Science, Banaras Hindu University, India and Wadia Institute of Himalayan Geology (WIHG), Dehradun, India. Polished thin section was coated with 20 nm thin layer of carbon for electron probe micro analyses using LEICA-EM ACE200 instrument. The CAMECA SXFive instrument was operated by SXFive Software at a voltage of 15 kV and

current 10 nA with a LaB6 source in the electron gun for the generation of an electron beam. Natural silicate mineral andardite as the internal standard used to verify positions of crystals (SP1-TAP, SP2-LiF, SP3-LPET, SP4-LTAP and SP5-PET) with respect to corresponding wavelength dispersive (WD) spectrometers (SP#) in CAMECA SXFive instrument. The following X-ray lines were used in the analyses: F-K α , Na-K α , Mg-K α , Al-K α , Si-K α , P-K α , Cl-K α , K-K α , Ca-K α , Ti-K α , Cr-K α , Mn-K α and Fe-K α . Natural mineral standards: fluorite, halite, apatite, periclase, corundum, wollastonite, orthoclase, rutile, chromite, rhodonite and hematite, supplied by CAMECA-AMETEK were used for routine calibration, X-ray elemental mapping and quantification. Routine calibration, acquisition, quantification and data processing were carried out using SxSAB version 6.1 and SX-Results software of CAMECA. The precision of the analysis is better than 1% for major element oxides and 5% for trace elements from the repeated analysis of standards. The analytical details are also given in Kumar et al. (2019, 2020).

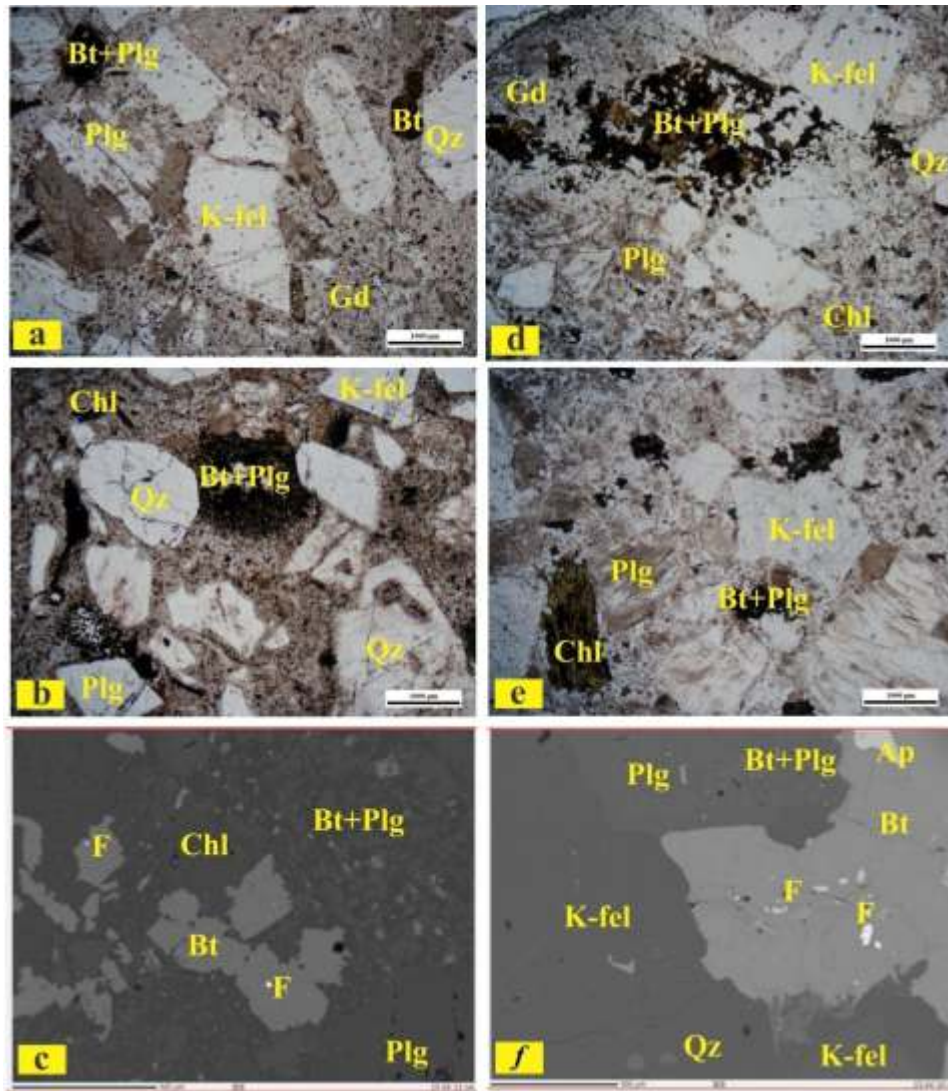


Fig. 3. (a) Riwasa rhyolite of grey variety showing porphyritic texture. (b) Vitrophyric texture present in Riwasa rhyolite of pink variety. (c) Back scattered electron (BSE) image recorded during EPMA shows rhyolitic texture with some halogen's content (fluorine and chlorine). (d) Granophyric texture present in Nigana granite of grey variety. (e) Hypidiomorphic texture present in Nigana granite of pink variety. (f) BSE image shows granitic texture of essential mineralogy with some halogens contents. Abbreviations used; Qz-quartz, Plg-plagioclase, K-fel-K-feldspar, Bt-biotite, Chl-chlorite, Ap-apatite, F-fluorine and Gd-groundmass.

4. Geochemical characteristics

The average geochemical data of the eight hills from Tusham Ring Complex is shown in Table 1. Geochemically, these acid volcano-plutonic rocks of peraluminous (Fig. 4a) and ferroan-enriched (Fig. 4b) nature display significant enrichment of SiO₂, Na₂O+K₂O, Fe/Mg, Rb, Th, U, Cu, Ga, Zn, Sn, W, Zr, Y and REE (except Eu); suggesting typical A-type affinity in extensional environment for TRC. Peraluminous A-type granitoids are corundum

normative and their high A/CNK (>1) ratio is consistent with magma derived from high-grade meta-sedimentary source (Eby and Kochhar, 1990). In chondrite normalized- and primitive mantle-normalized REE and trace element diagrams (Sun and McDonough, 1989), the granites and co-existing grey and pink rhyolites are very similar in chemistry and could be comagmatic (Fig. 4c & d). It is worth noting that all the rock samples have pronounced negative Eu anomaly (Eu/Eu*=0.13-0.47). The negative Eu anomaly

in the subsolidus to hypersolvus (peraluminous) granitoids could be due to interaction with a fluid phase and/or to fractionation of plagioclase (Eby and Kochhar, 1990). The slight HREEs enrichment in TRC granitoids may be due to F complex (Kumar et al., 2021). The mineral chemistry data (table 2 & table 3) also demonstrates that the feldspar (plagioclase and K-feldspar) (Fig. 5a) and biotite (phlogopite and annite) (Fig. 5b) played a significant role in the evolution of the rocks, which is in good agreement with the MIS petrography and mineralogy.

The acid volcano-plutonic rocks of the TRC were generated through partial melting of metasedimentary rocks of Delhi Super group and have undergone variable extents of fluids/melt-rock interactions, especially hydrothermal alteration and deposition of important rare metals (Kochhar, 1984; Sharma et al., 2019; Kumar et al., 2019, 2020). The high concentration of radioelements, i.e., U (4.2-14.3 ppm), Th (59.9-104.1 ppm) and K (5.0-6.2 wt%) and rare earth elements are strong indicators of high heat-producing and rare-metal bearing granitoids of the TRC. The conspicuous negative anomalies for Sr, P, Ti, Ba, and Eu on the multi-element diagram for studied granitoids are also common features for A-type granitoids (Whalen et al., 1987). The relative concentrations of Nb, Ce, Zr, Ga and Y are characteristics of their compatibility with a dominant crustal component in the magmatic melt (Eby, 1990). The elemental geochemistry i.e. elevated contents of HFSE, LILE and LREE in the studied granitoids is closely similar to the Mt. Abu granitoids, Erinpura granite and Nagarparkar granite (Fig. 4c & d). The Mt. Abu granitoids originated by partial melting and variable entrainment of peritectic reaction products such as clinopyroxene, plagioclase and ilmenite into the ascending magmas. However, the presence of prominent negative Eu anomalies, as well as the relative depletions in plagiophile elements like Sr and Ba, indicates substantial retention of plagioclase components in source materials during partial melting. Another possibility is that some of the chemical diversity in the studied granitoids might be produced by variable mixing with coeval mafic magmas which is also compatible to the Mt. Abu magmatic rocks (Ashwal et al.,

2013). The geochemical and petrogenetic evolutionary processes i.e. the partial melting, retention of plagioclase and variable mixing in the Mt. Abu granitoids are also quite similar to the TRC granitoids that were also objectives of previous study (Kumar et al., 2019, 2020). The magma related to Nagarparkar granitoids possessed crustal material, which leads to the enrichment of some incompatible trace elements and depletion of Sr and Ba in alkali feldspar-granites and relatively high Sr and Ba in biotite-granites, indicating a juvenile lower crust affinity (Shakoor et al., 2019). Furthermore, it was also suggested that Mt Abu granitoids are geochemically and petrologically distinct from Erinpura granitoids, but match those from the Malani Igneous Suite and Praslin Group granitoids of the Seychelles, which, along with northern Madagascar, formed now-fragmented components of an Andean-type magmatic arc on the margin of the Rodinia supercontinent (Ashwal et al., 2013). The REE pattern and primitive mantle pattern of Erinpura granite and Nagarparkar is also very similar to the TRC granitoids. But Erinpura granite was considered older than Malani felsic magmatism whereas the age, petrographical and geochemical characteristics of Nagarparkar and Mt. Abu matched with the adjacent Malani rocks (Ashwal et al., 2013; Shakoor et al., 2019).

The concentrations of trace and rare earth elements emphasize the role of halogens in fluxing these elements from the melt (Kochhar, 1984; Kumar et al., 2019; Sharma et al., 2019). The hydrous phases associated with these acid magmatic rocks are biotite and amphiboles. Biotite is highly enriched in Fluorine and Chlorine which confirm the halogen role in their magmatic evolution, LREE enriched and rare metal mineralization. Recently, Sharma et al. (2019) proposed that the TRC, being an extension of MIS, shows high heat production affinity, mineralization potential and A2-type geochemical nature. EPMA studies, carried out in various institutes, also provide new information regarding the role of halogens (especially, F and Cl), hydrothermal deposits (especially, porphyry copper deposits), rare metal affinity and fluid-rock interactions.

Table 1. The whole rock geochemical data set from Tusham Ring Complex (Northwestern peninsular India) and compiled with Mt. Abu, Erinpura and Nagarparkar granitoids.

Location	Riwasa		Nigana		Dharan		Dulheri		Khanak		Devsar		Dadam		Tusham		Mt. Abu		Erinpura		Nagarparkar	
	15	15	15	15	5	5	5	5	15	15	15	15	5	5	5	5	AA6-29	AA6-20	NP-01	NP-01		
Average data of selected samples from individual hill-lock																						
SiO ₂	73.0	71.5	67.9	69.9	68.4	69.4	69.5	64.7	75.0	71.4	74.3											
TiO ₂	0.2	0.3	0.4	0.4	0.5	0.4	0.4	0.3	0.3	0.5	0.2											
Al ₂ O ₃	12.9	13.5	15.0	14.6	14.6	14.8	15.7	19.8	12.0	13.8	11.6											
Fe ₂ O ₃	3.5	3.5	3.9	3.5	3.8	3.5	3.0	5.5	2.6	3.6	3.2											
MnO	0.1	0.0	0.1	0.1	0.1	0.1	0.1	0.0	0.1	0.1	0.1											
MgO	0.2	0.3	0.6	0.4	0.6	0.4	0.5	0.4	0.3	0.4	0.1											
CaO	1.0	1.4	1.9	1.5	1.7	1.4	1.3	0.1	1.1	1.4	0.3											
Na ₂ O	2.6	2.5	2.8	2.8	2.8	2.7	2.1	0.2	3.5	2.7	4.2											
K ₂ O	5.3	5.6	5.9	6.0	5.7	6.0	6.2	5.0	5.3	6.0	4.7											
P ₂ O ₅	0.0	0.1	0.1	0.1	0.1	0.1	0.1	0.0	0.1	0.1	0.1											
LOI	0.9	0.7	1.1	1.0	0.8	0.9	1.0	1.3	0.9	0.9	1.2											
Total	99.6	99.5	99.7	100.3	99.1	99.5	99.9	97.4	101.0	99.5	100.0											
Q	35.1	32.3	24.7	27.2	26.4	27.5	30.2	43.2	nc	27.5	nc											
Or	31.3	33.3	34.9	35.5	33.4	35.2	36.6	29.8	nc	35.2	nc											
Ab	22.1	21.1	23.4	23.4	24.0	22.9	18.0	2.0	nc	22.9	nc											
An	4.7	6.3	8.5	6.9	6.9	6.6	5.8	0.5	nc	6.6	nc											
Cor	1.2	1.0	0.9	1.0	1.3	1.4	3.4	13.8	nc	1.4	nc											
Hy	0.6	0.8	1.5	1.1	1.6	0.9	1.2	0.9	nc	0.9	nc											
Il	0.1	0.1	0.1	0.1	0.1	0.1	0.1	0.1	nc	0.1	nc											
Ap	0.1	0.2	0.3	0.3	0.3	0.2	0.3	0.1	nc	0.2	nc											
Hem	3.5	3.5	3.9	3.5	3.8	3.5	3.0	5.5	nc	3.5	nc											
Ru	0.2	0.3	0.5	0.4	0.5	0.4	0.4	0.4	nc	0.4	nc											

Sc	5.8	5.5	6.8	6.1	0.0	0.0	0.0	0.0	0.0	4.4	6.3	0.0
V	9.4	16.8	25.5	20.5	31.5	19.6	19.6	21.7	42.8	7.1	25.1	0.0
Cr	17.5	17.6	8.5	7.5	13.0	8.5	8.5	10.0	23.8	470.3	270.2	0.0
Ni	4.9	2.8	5.5	3.5	3.9	2.4	2.4	2.0	15.3	6.4	6.0	0.0
Cu	8.2	185.1	4.0	7.0	5.7	4.6	4.6	8.7	23.3	0.0	0.0	0.0
Zn	44.1	95.2	51.0	52.0	48.8	51.3	51.3	40.7	49.0	67.1	52.5	0.0
Ga	18.2	20.0	19.0	19.0	19.0	19.3	19.3	18.3	26.0	19.0	21.0	19.5
Rb	336.9	333.0	308.0	327.0	307.2	320.9	320.9	324.7	629.0	367.3	239.7	0.0
Sr	64.2	86.6	141.5	123.5	132.9	110.9	110.9	101.3	35.8	32.8	97.3	17.5
Y	58.4	55.3	52.0	55.0	51.7	53.6	53.6	47.3	79.3	110.6	37.1	107.0
Zr	208.6	259.9	299.5	246.0	301.4	305.1	305.1	262.3	177.8	203.2	300.9	727.0
Nb	21.6	21.6	22.5	22.0	25.2	19.9	19.9	17.7	114.0	33.3	17.8	29.9
Ba	597.8	729.7	935.0	909.0	922.7	926.6	926.6	807.7	201.8	207.6	528.0	168.0
Pb	49.6	42.3	37.5	47.0	31.1	45.8	45.8	28.0	47.3	47.4	49.2	0.0
Th	104.1	95.7	94.5	99.0	59.9	99.1	99.1	62.3	61.8	60.0	66.3	10.1
U	10.4	8.8	5.7	8.6	8.8	7.5	7.5	4.2	14.3	13.1	9.9	2.4
Ba/Rb	1.8	2.2	3.0	2.8	3.2	2.9	2.9	2.7	1.0	0.57	2.20	0.00
Rb/Sr	5.4	4.9	2.2	2.7	6.0	3.0	3.0	27.4	61.3	11.20	2.46	0.00
Rb/Ba	0.6	0.5	0.3	0.4	0.5	0.3	0.3	0.7	50.2	1.77	0.45	0.00
Ba/Sr	9.2	9.2	6.6	7.4	9.3	8.6	8.6	21.4	4.4	6.33	5.43	9.60
Th/U	10.4	11.4	16.7	13.2	10.1	14.1	14.1	9.2	4.4	4.58	6.70	4.26
La	282.1	245.1	177.5	183.6	143.9	210.3	210.3	130.3	44.9	98.2	80.3	5.0
Ce	555.1	475.3	327.5	339.7	268.9	390.3	390.3	253.9	98.0	204.6	187.5	148.0
Pr	60.0	50.8	35.8	36.9	29.9	41.8	41.8	27.5	12.1	24.3	18.9	17.5
Nd	193.1	163.8	118.9	122.0	101.5	136.8	136.8	93.4	43.6	88.8	67.2	68.8
Sm	30.5	25.1	18.4	19.1	17.9	22.8	22.8	17.0	13.1	18.1	11.6	16.1

Eu	1.8	2.2	2.4	2.1	2.8	2.5	2.8	0.6	1.2	1.3	1.2	1.2
Gd	29.0	23.9	19.1	19.9	17.0	21.1	15.3	15.0	19.0	11.4	19.0	16.1
Tb	3.7	2.9	2.4	2.5	2.3	2.7	1.9	3.3	3.1	1.4	3.1	3.0
Dy	17.9	13.6	12.5	12.8	11.6	12.7	9.2	21.7	18.7	7.2	18.7	18.8
Ho	3.5	2.6	2.5	2.5	2.5	2.7	1.9	5.5	3.9	1.3	3.9	4.0
Er	9.4	7.0	6.9	6.9	6.8	7.1	4.8	15.4	11.2	3.6	11.2	12.1
Tm	1.4	1.0	1.0	1.0	1.1	1.0	0.7	2.6	1.8	0.5	1.8	1.9
Yb	8.8	6.5	6.5	6.6	6.8	6.5	4.4	16.5	11.1	2.8	11.1	12.0
Lu	1.3	0.9	1.0	1.0	0.9	0.9	0.6	2.2	1.6	0.4	1.6	1.8
Σ REE	1197.6	1020.8	732.4	756.6	613.9	859.1	563.8	294.6	505.7	395.5	505.7	326.2
Σ LREE	1120.8	960.2	678.1	701.3	575.0	818.6	534.1	216.8	434.0	365.5	434.0	255.4
Σ HREE	74.9	58.4	51.9	53.2	49.0	54.6	38.9	82.2	70.5	28.6	70.5	69.6
	nc-not calculated		sample number (AA6-29)-Mt. Abu granitoid (Ashwal et al., 2013)									
			sample number (AA6-20)-Eripura granite (Ashwal et al., 2013)									
			sample number (NP-01)-Nagarparkar granite (Shakoor et al., 2019)									

Table 2. EPMA data of feldspar mineral from Tusham Ring Complex, southwestern Haryana, India.

Sample Points ID	RWN10 60/1	RWN10 61/1	RWN10 62/1	RWN20 63/1	RWN20 64/1	RWN41 65/1	NGN32B 70/1	NGN32B 71/1	NGN32B 75/1	NGN19 76/1	NIN30 85/1	NIN30 86/1	NIN2 87/2	NIN2/X 87/3	DUN2 91/1	DUN2 92/1
Oxides																
Na ₂ O	2.96	7.08	3.33	7.66	2.71	6.21	6.05	1.39	7.05	7.82	7.71	11.22	1.15	8.30	6.71	6.37
MgO	0.00	0.01	0.00	0.00	0.00	0.00	0.00	0.00	0.00	0.00	0.11	0.00	0.01	0.00	0.00	0.00
Al ₂ O ₃	18.61	24.07	18.50	24.33	17.72	26.12	26.33	17.91	24.72	24.34	23.38	18.76	17.95	23.49	25.45	26.62
P ₂ O ₅	0.01	0.00	0.00	0.02	0.00	0.02	0.00	0.00	0.08	0.04	0.00	0.01	0.01	0.00	0.02	0.03
Cr ₂ O ₃	0.00	0.00	0.01	0.00	0.00	0.00	0.00	0.00	0.00	0.00	0.05	0.00	0.00	0.00	0.00	0.00
MnO	0.00	0.00	0.00	0.00	0.09	0.05	0.03	0.00	0.00	0.00	0.00	0.00	0.00	0.00	0.00	0.00
CaO	0.22	6.51	0.28	6.57	0.16	8.83	9.29	0.06	5.78	6.26	4.80	8.01	0.09	5.70	7.92	8.91
K ₂ O	11.73	0.93	10.91	0.16	12.06	0.55	0.31	14.93	0.26	0.16	0.30	0.02	14.89	0.17	0.37	0.39
TiO ₂	0.02	0.02	0.06	0.02	0.00	0.00	0.00	0.00	0.00	0.00	0.00	0.06	0.11	0.01	0.02	0.00
FeO	0.28	0.26	0.14	0.22	0.30	0.05	0.21	0.07	0.00	0.00	0.10	0.02	0.10	0.11	0.03	0.12
SiO ₂	63.27	58.35	65.19	59.19	64.38	55.98	55.03	63.46	61.04	58.69	61.71	60.94	64.86	62.17	56.61	55.26
NiO	0.03	0.00	0.00	0.00	0.02	0.00	0.00	0.01	0.08	0.01	0.00	0.00	0.04	0.00	0.00	0.00
V ₂ O ₃	0.00	0.00	0.00	0.00	0.00	0.00	0.00	0.02	0.00	0.00	0.00	0.00	0.00	0.00	0.00	0.00
F	0.14	0.00	0.19	0.06	0.01	0.00	1.42	0.00	0.00	0.00	0.07	0.84	0.00	0.00	0.00	0.00
Cl	0.05	0.00	0.01	0.01	0.06	0.01	0.00	0.01	0.00	0.00	0.01	0.00	0.03	0.01	0.00	0.00
Total	97.32	97.23	98.63	98.23	97.52	97.81	98.67	97.89	99.01	97.31	98.24	99.89	99.23	99.96	97.12	97.70
Formula based on Oxygen 8 atoms																
Na	0.27	0.63	0.30	0.67	0.25	0.55	0.54	0.13	0.61	0.69	0.67	1.00	0.10	0.71	0.60	0.57
Mg	0.00	0.00	0.00	0.00	0.00	0.00	0.00	0.00	0.00	0.00	0.01	0.00	0.00	0.00	0.00	0.00
Al	1.03	1.30	1.00	1.30	0.98	1.41	1.44	1.00	1.30	1.31	1.24	1.01	0.98	1.23	1.38	1.45
P	0.00	0.00	0.00	0.00	0.00	0.00	0.00	0.00	0.00	0.00	0.00	0.00	0.00	0.00	0.00	0.00
Cr	0.00	0.00	0.00	0.00	0.00	0.00	0.00	0.00	0.00	0.00	0.00	0.00	0.00	0.00	0.00	0.00
Mn	0.00	0.00	0.00	0.00	0.00	0.00	0.00	0.00	0.00	0.00	0.00	0.00	0.00	0.00	0.00	0.00
Ca	0.01	0.32	0.01	0.32	0.01	0.43	0.46	0.00	0.28	0.31	0.23	0.39	0.00	0.27	0.39	0.44
K	0.70	0.05	0.64	0.01	0.72	0.03	0.02	0.90	0.01	0.01	0.02	0.00	0.88	0.01	0.02	0.02
Ti	0.00	0.00	0.00	0.00	0.00	0.00	0.00	0.00	0.00	0.00	0.00	0.00	0.00	0.00	0.00	0.00
Fe	0.01	0.01	0.01	0.01	0.01	0.00	0.01	0.00	0.00	0.00	0.00	0.00	0.00	0.00	0.00	0.00
Si	2.97	2.68	3.00	2.69	3.01	2.57	2.55	2.99	2.72	2.68	2.78	2.79	3.01	2.76	2.61	2.54
Ni	0.00	0.00	0.00	0.00	0.00	0.00	0.00	0.00	0.00	0.00	0.00	0.00	0.00	0.00	0.00	0.00
V	0.00	0.00	0.00	0.00	0.00	0.00	0.00	0.00	0.00	0.00	0.00	0.00	0.00	0.00	0.00	0.00
Total	5.00	5.01	4.96	5.00	4.98	5.01	5.02	5.02	4.93	5.01	4.95	5.20	4.99	4.99	5.01	5.03

Table 3. EPMA data of biotite mineral from Tusham Ring Complex, southwestern Haryana, India.

Sample Point	RWN10	RWN10	RWN41	RWN41/X	NGN32B	NGN32B	DUN2	DUN2	NGN19	NGN19/X	NIN30	NIN2/X	NGN32B/X	NGN32B/X	
ID	90/1	91/1	92/1	93/1	94/2	95/2	98/3	87/1	88/2	88/3	88/4	94/6	95/6	99/3	99/5
Na2O	0.28	0.09	0.11	0.02	0.17	0.14	0.10	0.13	0.17	0.21	0.16	0.08	0.02	0.08	0.06
MgO	4.20	3.58	3.04	3.59	5.10	5.19	5.27	5.09	9.66	11.21	2.95	3.30	2.87	4.54	4.99
Al2O3	12.39	11.97	12.60	12.17	12.56	12.76	11.30	11.61	12.32	12.40	13.30	13.10	13.69	11.96	12.32
P2O5	0.00	0.00	0.02	0.06	0.02	0.00	0.04	0.06	0.02	0.04	0.12	0.04	0.05	0.08	0.10
Cr2O3	0.09	0.06	0.08	0.07	0.06	0.04	0.00	0.02	0.00	0.01	0.00	0.04	0.08	0.13	0.12
MnO	0.65	0.44	0.61	0.56	0.28	0.34	0.58	0.44	0.23	0.33	0.45	0.33	0.52	0.47	0.45
CaO	0.16	0.21	0.07	0.04	0.04	0.01	0.01	0.04	0.16	0.00	0.02	0.11	0.09	0.08	0.04
K2O	9.01	7.85	8.55	8.92	9.03	9.18	8.95	9.08	9.58	9.33	8.90	8.70	9.07	9.39	9.03
TiO2	2.74	2.35	3.48	1.83	4.17	4.22	3.42	3.04	2.77	2.38	2.59	2.63	2.68	3.97	3.96
FeO	30.28	28.58	31.11	31.29	28.61	28.78	28.30	27.92	22.20	21.72	31.47	30.53	28.04	28.35	27.89
SiO2	34.36	34.78	33.94	34.38	34.24	33.95	35.54	34.68	35.28	34.73	33.44	34.39	34.59	34.60	35.01
NiO	0.09	0.00	0.19	0.17	0.00	0.00	0.00	0.04	0.12	0.08	0.00	0.00	0.08	0.13	0.00
V2O3	0.17	0.17	0.22	0.15	0.19	0.17	0.19	0.14	0.18	0.13	0.12	0.10	0.19	0.27	0.27
F	2.16	0.96	2.25	3.08	1.87	0.99	2.59	2.04	3.68	3.95	2.09	0.80	2.75	3.47	1.75
Cl	1.14	1.13	1.04	1.01	0.50	0.51	0.93	0.89	0.51	0.47	1.41	1.19	0.82	0.49	0.51
Sum	97.71	92.19	97.32	97.36	96.84	96.27	97.23	95.21	96.87	96.96	97.01	96.13	97.55	98.36	96.42
O=F, Cl	1.50	0.80	1.50	1.90	1.10	0.70	1.60	1.30	2.10	2.20	1.50	0.80	1.80	2.10	1.10
Formula based on Oxygen22															
Na	0.09	0.03	0.04	0.01	0.05	0.04	0.03	0.04	0.05	0.07	0.05	0.03	0.03	0.01	0.03
Mg	1.03	0.91	0.75	0.90	1.24	1.26	1.29	1.27	2.32	2.69	0.73	0.81	0.71	1.11	1.20
Al	2.41	2.40	2.47	2.41	2.42	2.45	2.19	2.28	2.34	2.36	2.62	2.64	2.57	2.64	2.31
P	0.00	0.00	0.00	0.01	0.00	0.00	0.01	0.01	0.00	0.01	0.02	0.01	0.01	0.01	0.01
Cr	0.01	0.01	0.01	0.01	0.01	0.01	0.00	0.00	0.00	0.00	0.00	0.01	0.01	0.02	0.01
Mn	0.09	0.06	0.09	0.08	0.04	0.05	0.08	0.06	0.03	0.05	0.06	0.05	0.07	0.06	0.06
Ca	0.03	0.04	0.01	0.01	0.01	0.00	0.00	0.01	0.03	0.00	0.00	0.00	0.02	0.02	0.01
K	1.90	1.70	1.81	1.91	1.88	1.91	1.87	1.93	1.97	1.92	1.90	1.82	1.92	1.96	1.90
Ti	0.34	0.30	0.44	0.23	0.51	0.52	0.42	0.38	0.34	0.29	0.33	0.31	0.33	0.33	0.49
Fe	4.18	4.07	4.32	4.39	3.91	3.92	3.88	3.89	3.00	2.93	4.40	4.14	4.25	3.84	3.89
Si	5.67	5.92	5.64	5.77	5.59	5.53	5.83	5.78	5.70	5.60	5.60	5.74	5.72	5.66	5.67
Ni	0.01	0.00	0.03	0.02	0.00	0.00	0.00	0.01	0.02	0.01	0.00	0.00	0.00	0.01	0.02
V	0.03	0.04	0.04	0.03	0.04	0.03	0.04	0.03	0.03	0.02	0.02	0.02	0.04	0.05	0.05
Fe++	1.05	1.02	1.09	1.10	0.98	0.99	0.98	0.98	0.75	0.74	1.11	1.04	1.07	0.96	0.96
Fe+++	2.10	2.05	2.17	2.21	1.96	1.97	1.95	1.96	1.51	1.47	2.20	2.08	2.14	1.93	1.91
Total	15.80	15.48	15.65	15.77	15.69	15.73	15.64	15.69	15.84	15.94	15.74	15.56	15.67	15.70	15.61

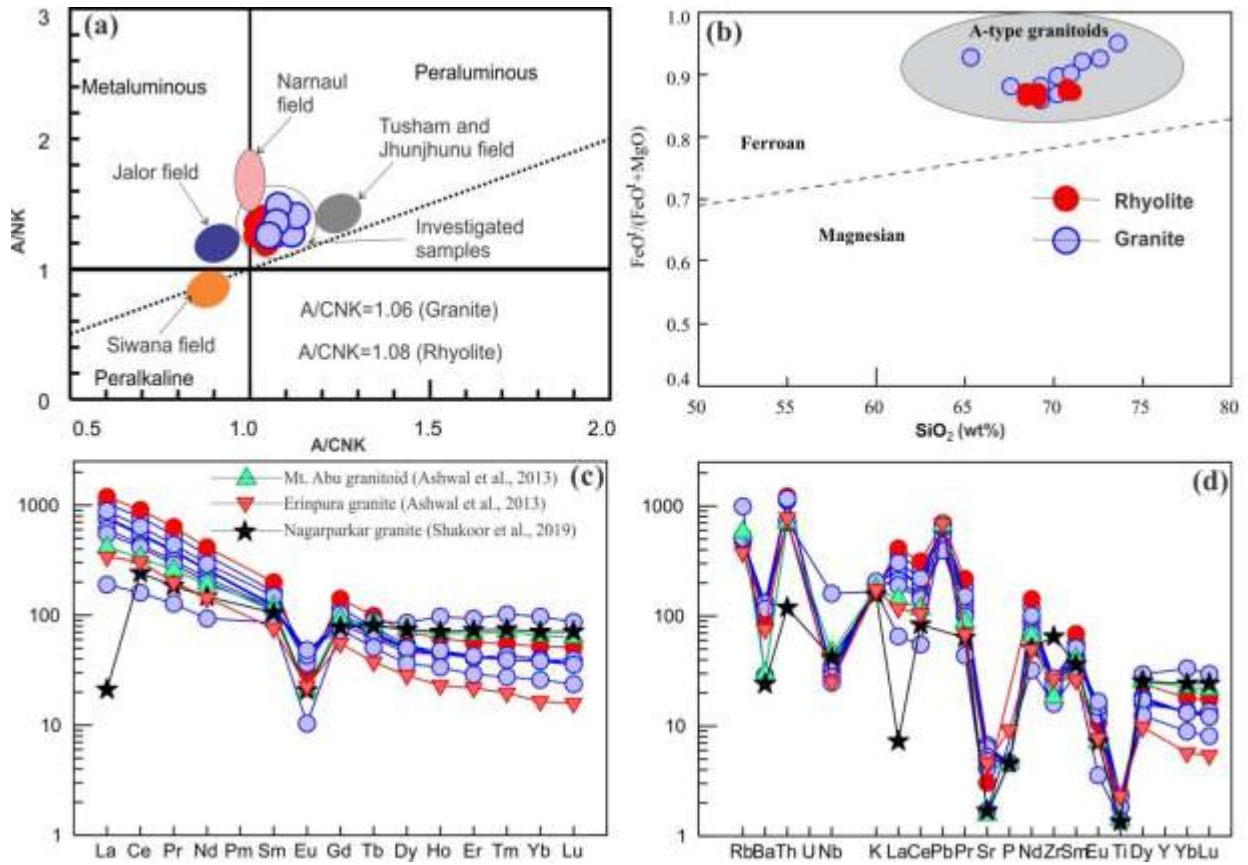


Fig. 4. (a) A/NK vs A/CNK plot of the analyses from TRC. For comparison are plotted other MIS rock-Siwana, Jalor, Jhunjhunu, and Narnaul fields (Delhi Supergroup). The TRC rocks plot in peraluminous field. (b) SiO₂ versus FeO_t/(FeO_t+MgO) diagram displays ferroan enriched A-type granitoids nature of TRC rock-suites (after Frost et al., 2001). (c) Chondrite normalized-spider diagram, (d) rock/primitive mantle diagram constructed for rhyolites and co-existing granites of the investigated areas, suggesting co-magmatic nature of their evolution (normalizing values after Sun and McDonough, 1989). Mt. Abu granitoid, Erinpura granite and Nagarparkar granite fields are plotted for geochemical comparison.

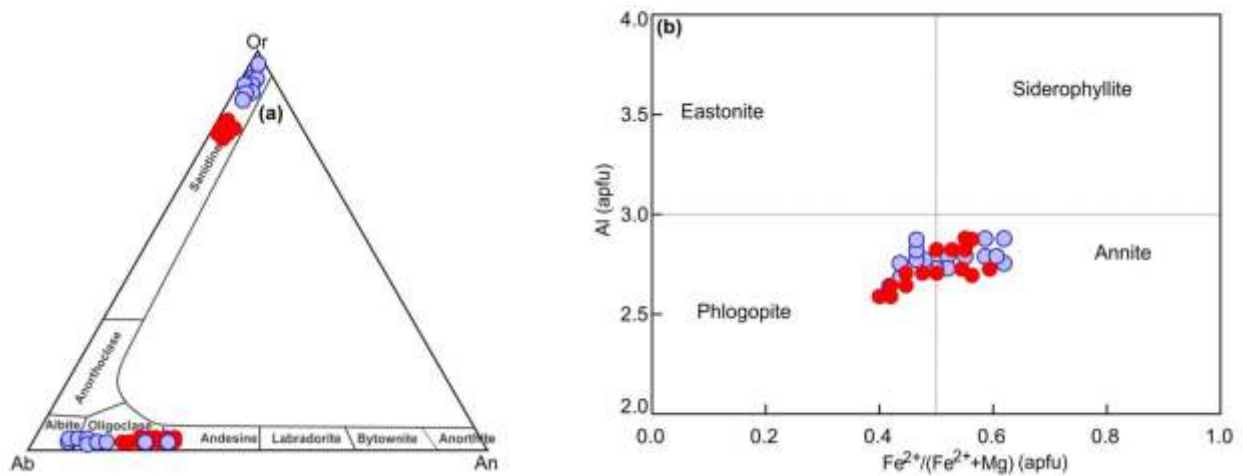


Fig. 5. (a) Ab-Or-An triangular diagram shows orthoclase and sanidine are important alkali feldspar and albite, oligoclase and andesine are important plagioclase feldspar as rock-forming minerals in TRC. (b) Fe²⁺/(Fe²⁺+Mg) (apfu) versus Al (apfu) binary plot indicates phlogopite and annite are important biotite minerals in the rocks. Dots are rhyolites and circles are granites.

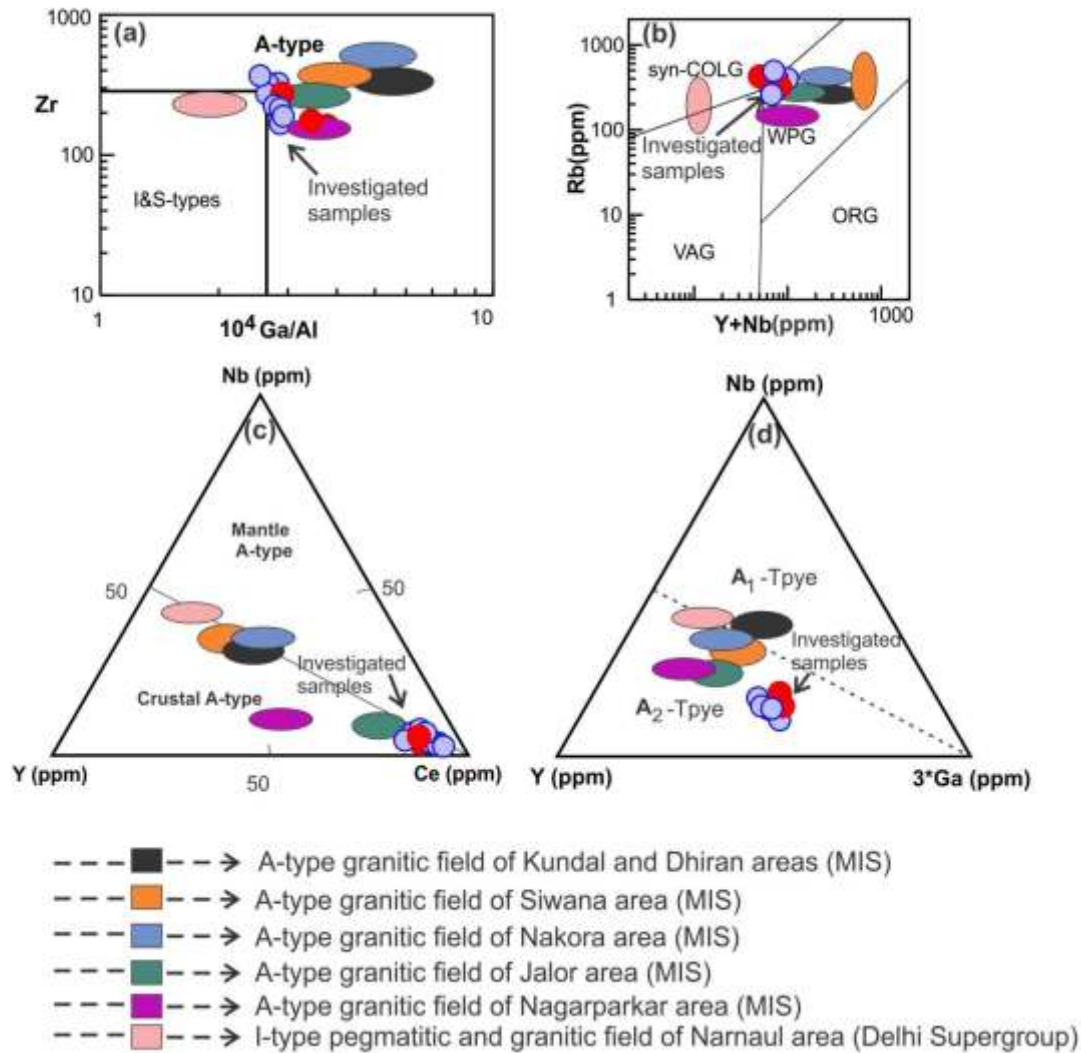


Fig. 6. (a) Plot of analyses from various granitoid bodies of the MIS in 10^4 Ga/Al vs Zr diagram shows A-type affinity (after Whalen et al., 1987). (b) Y+Nb vs Rb diagram suggest that these rocks are formed in within-plate granite setting (after Pearce et al., 1984). (c) Triangular diagram (Nb-Y-Ce) relations suggest essentially crustal source for the rocks (Eby, 1992). (d) Plots of the analyses on Nb--Y-- 3^* Ga diagram of Eby (1992) shows that the investigating rock of TRC belong to A₂-type granitoids. Kundal, Dhiran, Siwana, Nakora, Jalor, and Narnaul fields (Delhi Supergroup) are plotted for comparison.

5. Discussion

Some important aspects relevant to the present and previous works are discussed below;

5.1. Magmatic evolution

A variety of geotectonic models has been proposed for the origin of A-type granitoids and their sub-types (A₁ & A₂). It has been proposed that A₁ and A₂ groups have different sources and geodynamic settings. Eby (1992) suggested that A₁ group is formed from differentiation of magma derived from oceanic-island type basalt

emplaced in continental rifts (intraplate magmatism), whereas A₂ group formed from magma derived in continental crust or underplated crust which manifested continent-continent collision or island arc type of regimes (Eby, 1992). Based on the petrological and geochemical dataset, it was concluded that the acid volcano-plutonic rocks of TRC and MIS were also generated through partial melting (low to high degree) of crustal rocks (Pareek, 1981; Kochhar, 1984; Sharma and Kumar, 2017; Kumar et al., 2019, 2020). More importantly, the heat required for the melting process was supplied by mantle plume. Based on the above

discussion, it can be predicted that the magmatic evolution of the investigating granitoids (member of A2 group) was controlled by variable degree of partial melting of continental crust.

5.2. Petrogenetic aspects and relevant models

Alkaline magmatism may occur in tensional tectonic environment and can overlap with latest orogenic intrusions (Bonin, 1990) and late phases of arc magmatism. However, the nature of magma source rocks which are undergoing partial melting play an important role in producing the parental magma. Two different tectonic models have been proposed for the geodynamics of Neoproterozoic Malani Igneous Suite, i.e., plume related extensional model (Kochhar, 1984; Kumar et al., 2020) and Andean type subduction model (Ashwal et al. 2013). The currently preferred model for the evolution of orogenic to anorogenic alkaline magmas in TRC is strongly consistent with the partial melting of crustal rocks and hybridized mantle as heat supplier in melting process. In partial melting zone, water solubility favors batch melting of source magma which generates orogenic rock-suite and dehydration of source magma results into anorogenic in same period of time (Bonin, 1990). This can be considered that post-orogenic alkaline granites are the first to be emplaced and are followed by early anorogenic granites. Peraluminous complexes have been interpreted as evidence for crustal contamination from leaching of the calc-alkaline basement by hydrothermal fluids and percolating activity through melts or consolidated rocks (Bonin, 1987). A-type granitoids include anorogenic granites in rift-related and stable continental zones which are mildly alkaline in nature and crystallized from magma low in H₂O and O₂ fugacities with high HF/H₂O ratios (El Dabe, 2013). MIS is also considered as postorogenic category of A-type granitoids (see table of El Dabe, 2013) which were emplaced in post subduction setting (El Dabe, 2013). Many orogenic belts represent associations of calc-alkaline and alkaline igneous centers which are closely related in space and time.

Further, it was evident that the acid volcano-plutonic rocks of TRC were generated from halogen-enriched magmatic source with low degree of partial melting of continental crust

(Kumar et al., 2021). Based on binary and ternary diagrams (Fig. 6a-d), it is very clear that the investigated granitoids of TRC region are of A-type affinity, crustal derived and were emplaced nearby within-plate to volcanic arc of A2-type post-collisional tectonic regimes. Elemental geochemistry also attests that the granitoids represent genetically related post-collisional A2-type rocks with higher values of Heat production (HP), Heat Generation Unit (HGU) and radioelement concentration (Ur). Further, our new results are justified with the statement i.e. granitoids having Y/Nb ratio ($1 < Y/Nb < 4$), with sodic and potassic affinities showing medium to high FeOt/MgO values display reduced Rift related granitoids regime (El Dabe, 2013).

5.3. Tectonic implications

The anorogenic, postorogenic and alkaline groups of A-type granitoids are distinguished into hotspot, rift and post continent-continent collision, post-subduction magma regimes and island arc-typology respectively. The magma generated by hot spot activity has the highest differentiated index (DI) values with respect to other tectonic settings (El Dabe, 2013). Our new results of field, petrography, petrological and geochemical characteristics, in conjunction with geodynamic evolution of the TRC granitoids, indicate complex tectonic environment, i.e., orogenic to anorogenic tectonic-magmatic activities are possible around TRC with respect to the Malani Supercontinent. This statement is in good agreement with the anorogenic Neoproterozoic magmatism of TRC was exposed just after the orogenic activities of Proterozoic Aravalli magmatism. The emplacement of TRC granitoids can be subdivided into two groups on the basis of orogenic and anorogenic tectonic activities:

(1) Post-orogenic: Ba and Sr-rich granitoids (all granitic massifs of TRC except Tusham and Riwasa volcanics) having peraluminous characters emplaced in late-orogenic formations i.e. at the ending point of Aravalli magmatism of orogenic movement. The terminal stage of Delhi orogeny is marked by felsic magmatism i.e. Erinpura granitoids. So, the genesis of granitic massifs of TRC might be younger than Erinpura granitoids. Erinpura was the earliest rift magmatism which was considered >100 Ma

older than Tusham.

(2) Early anorogenic: Ba and Sr-poor grayish to pinkish hypersolvus granitoids (Riwasa and Tusham volcanic) having Fe-rich mafic mineralogy with low contents of Mn which promote hydrothermal alterations. The volcanic phase is considered as early phase of MIS magmatism which also coincided with the starting of anorogenic activities in NW Indian shield.

This transition period is very unique in geological history which portrayed both characters (orogenic to anorogenic) in exposed rock-types. The idea is fully based on experimental studies which include geological, petrological and geochemical data bank that will promote a new petrogenetic model of complex framework in TRC (Kumar et al., 2020).

5. Conclusion:

- (a) The present investigation has concluded that rocks exposed in Tusham Ring Complex were formed in confusing geological environment in which magmatic rocks show both anorogenic and orogenic characters.
- (b) They are typically represented by high alumina, iron with different major and trace elements concentration i.e. comagmatic magma might be generated through different source/variable degree of partial melting.
- (c) The role of halogens (especially, F and Cl) indicate that external fluid played an important role in their formation and also in hydrothermal activity around TRC (case of metallogeny). It can be concluded that the studied granitoids having A2-type affinity were generated from halogen-enriched magma.
- (d) The field, petrography, geochemistry and tectonic affinity suggest that A2-type acid volcano-plutonic rock-types under investigation have close linkage with the Malani Supercontinent and were generated through complex geological processes.

- (e) The mineral chemistry data also demonstrates that the feldspar (plagioclase and K-feldspar) and biotite (phlogopite and annite) played a significant role in the rock-forming processes of A2-type granitoids as similar to MIS.

Acknowledgement

The authors wish to express their thanks to Dr. A.R. Chaudhri (Department of Geology, Kurukshetra University, Kurukshetra, India) and Dr. Kalachand Sain (Wadia Institute of Himalayan Geology, Dehradun, India) for their support. We are thankful to Professor Dr. N.V. Chalapathi Rao and Dr. Dinesh Pandit of Banaras Hindu University, Varanasi, India, for their assistance to carry out the EPMA analysis. We are indebted to Dr. Naresh Kochhar (Punjab University, Chandigarh), Dr. R. K. Bikramaditya Singh (Banaras Hindu University, Varanasi, India) and Dr. A. Krishnakanta Singh (Wadia Institute of Himalayan Geology, Dehradun, India) for their valuable suggestions. Many thanks to two anonymous reviewers (especially, Professor Dr. M. Qasim Jan) for their valuable comments and suggestions for improvement of the final manuscript. Great thanks go to Dr. M. Younis Khan for managing the manuscript.

Funding

The first author wishes to acknowledge the financial support of the Junior Research Fellowship, University Grand Commission, New Delhi (India) to carry out the research work.

Authors' Contribution:

Naveen Kumar, proposed the main concept and involved in write up. He collected field and geochemical data sets under the supervision of Naresh Kumar. Naresh Kumar helped in the provision of relevant literature, review and preparation of illustration of figures and geochemical interpretation of the rocks under study.

References

- Ashwal, L.D., Solanki, A.M., Pandit, M.K., Corfu, F., Hendriks, B.W.H., Burke, K., Torsvik, T.H., 2013. Geochronology and geochemistry of Neoproterozoic Mt. Abu

- granitoids, NW India: Regional correlation and implications for Rodinia paleogeography. *Precambrian Research*, 236, 265-281.
- Bonin, B., Platevoet, B., Vailette, Y., 1987. The geodynamic significance of alkaline magmatism in the western Mediterranean compared with West Africa. *Geological Journal*, 22, 361-387.
- Bonin, B., 1990. From orogenic to anorogenic settings: Evolution of granitoid suites after a major orogenesis. *Geological Journal*, 25, 261-270.
- Crawford, A.R., Compston, W., 1970. The age of Vindhyan system of peninsular India. *Journal of Geological Society London*, 175, 351-370.
- Eby, G.N., 1990. The A-type granitoids: A review of their occurrences, chemical characteristics and speculations on their petrogenesis. *Lithos*, 26, 115-134.
- Eby, G.N., 1992. Chemical subdivision of A-type granitoids: petrogenesis and tectonic implications. *Journal of Geology*, 20, 641-644.
- Eby, G.N., Kochhar, N., 1990. Geochemistry and petrogenesis of the Malani Igneous Suite, North Peninsular India. *Journal of the Geological Society of India*, 36(2), 109-130.
- El Dabe, M.M., 2013. A geochemical tectonomagmatic classification of the A-type granitoids based on their magma types and tectonic regimes. *Journal of Arabian Geosciences*, 8, 187-193.
- Frost, B.R., Barnes, C.G., Collins, W.J., Arculus, R.J., Ellis, D.J., Frost, C.D., 2001. A geochemical classification for granitic rocks. *Journal of Petrology*, 42, 2033-2048.
- Kochhar, N., 1984. Tusham Ring Complex, Bhiwani, India. *Proceedings of Indian Natural Science Academy*, 49, 459-490.
- Kochhar, N., 2015. The Malani Supercontinent. *Frontiers of Earth Sciences*, 120-135.
- Kumar, N., Kumar, N., Singh, A.K., 2019. Petrology and Geochemistry of Acid Volcano-Plutonic Rocks from Riwasa and Nigana Areas of Neoproterozoic Malani Igneous Suite, Northwestern Peninsular India: An Understanding Approach to Magmatic Evolution. *Geochemistry International*, 57, 645-667.
- Kumar, N., Kumar, N., Sharma, R., Singh, A.K., 2020. Petrogenesis and tectonic significance of the neoproterozoic magmatism of the Tusham Ring Complex (NW Indian Shield): Insight into tectonic evolution of the Malani Igneous Suite and Rodinia Supercontinent. *Geotectonics*, 54, 428-453.
- Kumar, N., Kumar, N., Sharma, R., Singh, A.K., 2021. Geochemical characteristics of fluorine-and chlorine-bearing biotite from Tusham Ring Complex, NW India: Constraints on halogen distribution and geodynamic evolution, *Journal of Earth System Science* (in press).
- Pareek, H.S., 1981. Petrochemistry and petrogenesis of the Malani igneous suite, India, *Geological Society of American Bulletin*, 92, 67-70.
- Pearce, J.A., Harris, N.B.W., Tindle, A.G., 1984. Trace element discrimination diagrams for the tectonic interpretation of granitic rocks. *Journal of Petrology*, 25, 956-983.
- Shakoor, M.A., Yang, X., Deng, J., Hakro, A.A.D., 2019. Early Neoproterozoic evolution of Southeast Pakistan: evidence from geochemistry, geochronology, and isotopic composition of the Nagarparkar Igneous Complex. *International Geology Review*, 61, 1391-1408.
- Sharma, R., Kumar, N., 2017. Petrology and geochemistry of A-type granites from Khanak and Devsar areas of Bhiwani district, southwestern Haryana. *Journal of the Geological Society of India*, 90 (2), 138-146.
- Sharma, R., Kumar, N., Kumar N., 2019. Signatures of high heat production and mineralization associated with plutonic and volcanic acidic rocks from Tosham Ring Complex, Southwestern Haryana, India. *Himalayan Geology*, 40 (2), 239-247.
- Sun, S.S., McDonough, W.F., 1989. Chemical and isotopic systematics of oceanic basalts: Implications for mantle composition and processes. *Geological Society London Special Publications*, 42, 313-345.
- Wang, W., Cawood, P.A., Zhou, M-F., Pandit, M.K., Xia, X-P., Zhao, J-H., 2017. Low- $\delta^{18}\text{O}$ Rhyolites from the Malani Igneous Suite: A Positive Test for South China and NW India Linkage in Rodinia. *Geophysical Research Letters*, 44(10),

298-305.

Whalen, J.B., Currie, K.L., Chappell, B.W.,
1987. A-type granites: Geochemical
characteristics, discrimination and
petrogenesis. *Contributions to mineralogy
and petrology*, 95, 407-419.